Astron. Astrophys. 274, 465–477 (1993)

ASTRONOMY AND ASTROPHYSICS

Complex structure in two diffuse interstellar bands

P. Jenniskens[1] **and F.-X. Désert**[2,3]

[1] Leiden Observatory, P.O. Box 9513, NL-2300 RA Leiden, The Netherlands
[2] DEMIRM, Observatoire de Meudon, F-92195 Meudon Cedex, France
[3] Institut d'Astrophysique Spatiale, Bat 121, Université Paris XI, F-91405 Orsay Cedex, France

Received November 5, accepted November 20, 1992

Abstract. The two strongest diffuse interstellar bands in terms of depth, those at 5780 Åand 6284 Å, show a complex shape with significant structure. In particular, many new weak features are clearly detected at irregular intervals superposed on a background absorption.

These features are tentatively assigned to either the main diffuse band (λ5780, λ6284) or to the nearby bands λ5797 and λ6296 respectively, which belong to a different family. All features that correlate well with the main bands form a complex profile. The shapes of these complex bands at 5780 and 6284 Å, including the asymmetries in the features, show some striking similarities (Fig. 10). This reduces the likelyhood that the features are merely a chance superposition of unrelated absorptions. The main bands are well correlated and could come from the same carrier.

Possible interpretations of the complex structures are given, assuming that (large) unidentified molecules are the carriers.

Key words: dust – extinction – diffuse interstellar bands – interstellar medium

1. Introduction

Diffuse interstellar bands (DIB) are unidentified broad absorption bands usually observed in the visual and near infrared spectra of reddened early type stars. These absorptions have their origin in the interstellar medium between the star and the observer and not in the atmosphere of the star (Merrill 1936). Today more than 100 DIBs are known (Herbig & Leka 1991), but in spite of their considerable history in observational astronomy (Bromage 1987) none of the DIBs has been identified.

Most absorption bands have a full width at half maximum ($FWHM$) in the range 0.7 - 3 Å (2-10 cm^{-1}), but there is a class of bands that are as broad as $FWHM \sim 20$ Å. All bands are always broader than expected from the Doppler broadening of turbulent motions in the interstellar clouds (typically < 0.1 Å) and broader than the sharp absorption lines of simple atomic and diatomic molecules such as CH and CN. This large width and the position of the bands in the visual part of the spectrum point towards two possible origins: 1) vibronic transitions in large gas-phase ions or radicals and 2) impurity absorptions in small solid grains (for a review see: Bromage 1972; Smith et al. 1977; Van der Zwet 1987).

Diffuse bands are mostly regarded as featureless Gaussian or Lorentzian profiles. Although expected at some level (Danks & Lambert 1976; Cossart–Magos & Leach 1990), no rotational or vibrational structure has so far been found in high resolution spectra of DIBs (Danks & Lambert 1976; Snell & Vanden Bout 1981; Hayden–Smith et al. 1981; Herbig & Soderblom 1982), although asymmetries have been observed (e.g. Wu 1972; Savage 1976). Significant profile variations from one line of sight to another have been reported by Snell & Vanden Bout (1981) for λ5780. These variations could be due to an unrelated absorption feature.

Several authors have tried to relate diffuse bands with each other. Herbig (1975) found from his DIB catalogue that in 7 cases, broad and narrow features are found in pairs, but discarded the resemblance to an unresolved molecular band because the asymmetry in the sharp lines did not agree with that. Correlation studies of band strenghts in a range of lines of sight has led to the recognition of families of bands (Chlewicki et al. 1986; Krelowski & Walker 1987), which are defined as groups of bands of which the strengths correlate better within a group than with other families. For example, λ5780 and λ6284 are in the same family. There is some confusion about the family assignment for many other bands (compare Krelowski & Walker 1987 with Josafatsson & Snow 1987). Within the families there is no clear pattern in the frequencies at which the lines are found. A more or less regular pattern was found by Herbig (1988) from a cluster of weak DIBs between 6780 and 6860 Å. Five of the stronger bands are found to be more or less equally spaced by about 100 cmcm^{-1}.

The aim of this work is to show that there is a significant structure in the profiles of the λ5780 (Sect. 3) and λ6284 DIBs (Sect. 4) and their broad associated bands. These are the two strongest DIBs in terms of depth and, consequently, it is possible

Send offprint requests to: P. Jenniskens, NASA/Ames Research Center, Mail Stop 239-4, Moffett Field, CA94035-1000, USA.

to obtain high S/N in the feature in reasonable integration times. The similarity found in the shape of both profiles (Sect. 5) argues against a chance superposition of weak unrelated DIBs. In (Sect. 7) the possible explanations of such a complex structure are discussed.

We follow Herbig's notation by indicating each individual DIB by the symbol "λ" followed by the laboratory rest wavelength in air (in Å), for example λ5780. According to convention, wavenumbers ($\nu = \lambda^{-1}$, in cm^{-1}) are given in vacuum, where $\nu = \lambda_{air}^{-1}/1.000276$. All spectra are shown in terms of transmittance, given as $F_\lambda = I(\lambda)/I^o(\lambda)$.

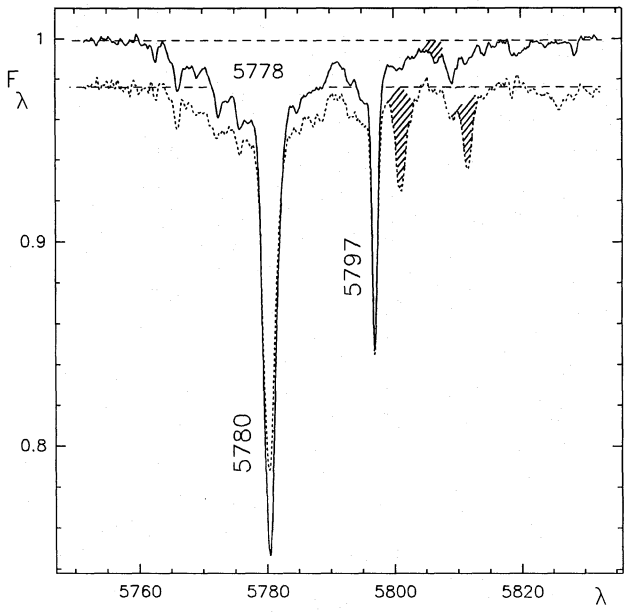

Fig. 1. The complexity of the DIBs near λ5780 and λ5797 is shown in this set of average spectra of several B stars (upper curve) and several O type stars with similar rotational velocity (lower curve, shifted downward slightly). The difference in stellar type results in a different set of stellar atmosphere lines in the spectra (hatched)

2. Data analysis

2.1. Observations

The data consist of yellow and red spectra of reddened early type stars obtained at the 1.52m f27.6 Coude telescope at the *Observatoire de Haute Provence* (O.H.P.), France. 31 program stars were initially selected for a DIB study that is reported elsewhere in order to represent a wide variety of lines of sight (Désert et al. 1993). They cover the range in E_{B-V} of 0.0 - 1.3 mag. and are of spectral type A0 to O4.

The spectrometer "Aurelie" (Gillet 1990) was set to a FWHM resolution of 0.3 Å with three pixels per resolution element, i.e. 0.1 Å/px. The detection and readout system is split : a linear Reticon array of 2048 diodes is read by two 1024 pixel CCDs. This surpresses ghost images from strong features in the spectra. The system covers a wavelength range of 200 Å, centered in the yellow at 5770 Å for the strong λ5780 and λ5797 DIBs and in the red at 6240Å to cover the strong λ6284 and λ6269 DIBs along with the associated shallow features. Each spectrum was corrected for pixel–to–pixel offset and gain variations. We used the whole spectrum for a first or second order baseline calibration, which puts the continuum in each spectrum at 1.0 and leaves negligible remaining curvature in the spectra. Here, we present only the wavelength ranges from 5750 to 5830 Å (the 5780 window) and from 6220 to 6340 Å (the 6284 window), because they are relatively free of stellar lines.

The wavelength scale is corrected for Doppler motion of the interstellar matter relative to the observer by aligning the central positions of Gaussian profiles fitted to the strong λ5797 and narrow λ6195 with the laboratory rest wavelengths of 5797.06 $\pm$0.05 and 6195.95$\pm$0.05 Å respectively.

These values were derived from the relative position of the interstellar absorption lines of CH (4300.31 Å), CaII (3933.66 and 3968.47 Å) and NaI (5889.95 and 5895.92 Å) towards the stars HD183143, HD30614 and HD190603, and are in good agreement with Wallerstein (1974), who has 5797.08 $\pm$ 0.20, Herbig (1975), who finds 5797.03 $\pm$ 0.02 and 6195.95 $\pm$ 0.02 respectively, and Benvenuti & Porceddu (1989), who find 5797.06 $\pm$ 0.07 and 6195.89 $\pm$ 0.05. All previous data are from a comparison with NaI lines only.

2.2. Sources of contamination

Stellar photospheric lines, telluric absorptions and detector pixel to pixel sensitivity variations contaminate the spectra. They were carefully removed (telluric absorptions) or are marked in the spectra.

Weak stellar lines were detected from a series of spectra of unreddened stars and identified from the multiplet tables of Moore (1945). These unreddened stars are HD34087 (O9Ve), 214680 (O8III), 37742 (O9Ib), 205021 (B2III), 34085 (B8Iae), 32630 (B3V), 47839 (O7V), 199081 (B5V) and 22928 (B5III). The following stellar lines were found. The 5780 window contains an unidentified stellar line at 5771.5 Å, which is strong in HD214680 and HD34087 (O super giants). A weak NII line is found in HD205021 at 5767.43 Å. The CIV doublet at 5801.51 and 5812.14 Å is strong in O type stars. In late B type supergiants, lines of SiII are found at 5800.48, 5806.75 and 5827.80 Å. Two unidentified lines are found at 5819.3 (weak) and 5833.45 (strong in HD205021) in B type stars. In the 6284 window there is a strong line of NeI at 6266.50 Å and a line at 6305.51 Å of possibly SII in late B type giants. Several weak stellar lines of FeII (6238.38, 6239.36, 6239.95, 6247.56, 6248.92), NII (6242.52, 6284.30), and SII (6274.34, 6286.35, 6287.06) cause an apparent increase of noise in the continuum. In some O type stars, broad HeII lines are found at 6233.8 and 6310.8 Å.

Detector features can be recognized by recording the same spectrum twice with a significant shift in wavelength. One third of our 22 program stars, with reddenings varying from 0.3 to 1.28, were recorded with a shift of 2 Å (20 pixels). There are some weak remnants at 5764.8, 5775.5 and 5780.4 Å and a sharp

spike at 5783.4 Å. The relative intensity of these features does not vary from spectrum to spectrum, but the absolute intensity does. The features are weak and are not apparent in the figures shown here.

The telluric absorptions of oxygen and water were removed by observing the B3V standard star η UMa (E_{B-V} =0.01, V=1.8 mag.), which has broad stellar lines due to fast rotation of the star. The corrected spectrum (I_c) equals:

$$I_c = \frac{I}{I_{ref}^{\alpha}} \qquad (2)$$

where the exponent α is found iteratively starting from the ratio of optical depths of the strongest telluric features in the unreddened and reddened star spectra. There are a number of weak telluric lines of oxygen and water near 5790Å (see Westerlund & Krelowski 1988) and the strong $b^1\Sigma_g^+ - X^3\Sigma_g^-$ system of oxygen has a band head at 6276 Å. These can be removed down to the point where only some excess noise is left, because the bands are nearly resolved and the spectrum does not vary much from one direction to another (e.g. Benvenuti & Porceddu 1989). On the other hand, water features are less well dealt with, because the telluric water spectrum as well as the total intensity vary slightly even for constant elevation on the sky. Fortunately, the observed spectral range does not have strong water absorption features.

3. The 5780 window

3.1. New diffuse interstellar bands

Four DIBs in this spectral window are well established (Heger 1921; Merril 1936; Herbig 1975): λ5780, λ5797, the broad λ5778 and the background feature to λ5797, to which we will refer as λ5796. We find a number of new sharp features, notably on the short wavelength side of λ5778. Figure 1 shows two spectra with S/N=450 and S/N=270 per pixel of 0.1 Å, respectively, which are a weighted average of several B–type and O–type stars. Note the differences in stellar line content (hatched).

Our first approach is merely to identify all peaks in the absorption profile as individual DIBs. In order to be diffuse interstellar bands, the new features should follow the criteria of Herbig (1975):

1. They are found in the spectra of both reddened O and B type stars (Fig. 1).
2. The FWHM does not vary for lines of sight towards stars with differing stellar rotational velocities (except if there is significant spread in the relative velocity of interstellar matter). This criterium is clearly met by the fast rotating star HD217086 (Fig 2.): while the stellar lines are broadened to the point that they form a continuum, the narrow DIB candidates stand out clearly.
3. The features should follow the Doppler velocity of the interstellar clouds in the line of sight, i.e. λ5797, and not the stellar radial velocity (the difference is about 2 resolution elements, 0.7 Å, in the extreme cases).
4. The strength of the DIBs increases roughly with E_{B-V}, although there is considerable intrinsic scatter (Snow 1973; Herbig 1975).

Table 1. Rest wavelength (in air), rest frequency (in vacuum), FWHM, equivalent width, and peak optical depth of the individual features that make up the complex DIB around 5780 Å in the star HD183143. For the features indicated with an asterix a non-DIB origin is unlikely but not completely ruled out. Herbig's denomination is in the last column. a) Position from data of Snell & Vanden Bout (1981).

	λ_c (Å)	ν (cm^{-1})	FWHM (Å)	W (mÅ)	A_c	notes
1.	5762.7*	17348.2	0.7	14	0.019	
2.	5766.1	17337.9	1.3	32	0.027	
3.	5769.1	17328.9	0.8	4	0.010	
4.	5772.4	17319.0	1.1	44	0.026	
5.	5773.9*	17314.5	-.-	—	0.005	
6.	5775.8	17308.8	1.0	23	0.017	
7.	5777.3*	17304.3	-.-	–	0.005	
8.	5779.6[a]	17297.4	-.-	–	-.—	shoulder
9.	5780.0	17296.2	13.	840	0.061	=λ5778
10.	5780.42	17295.0	2.2	720	0.311	=λ5780
11.	5784.9	17281.6	1.0	10	0.010	
12.	5787.5	17273.8	1.0	7	0.010	
13.	5788.8	17269.9	1.0	23	0.010	
14.	5793.2	17256.8	1.1	9	0.011	
15.	5795.5	17250.0	1.0	–	0.014	
16.	5796.5	17247.0	4.5	190	0.039	=λ5796
17.	5797.03	17245.4	0.98	178	0.173	=λ5797
18.	5800.8*	17234.2	1.0	6	0.007	
19.	5806.6*	17217.0	1.0	–	0.010	
20.	5809.2	17209.3	1.0	20	0.019	
21.	5811.7*	17201.9	2.1	–	0.019	
22.	5814.3	17194.2	0.7	8	0.011	
23.	5818.6	17181.5	0.6	4	0.007	
24.	5828.5	17152.3	0.6	6	0.009	

Table 1 summarizes the parameters describing the individual features in the spectrum of HD183143 that we have identified as DIBs. Some identifications of weak (and stellar line contaminated) lines are less certain than others, and these are indicated by an asterix. The values for the equivalent widths and the other parameters can be compared with other DIB values found e.g. by Herbig (1975, 1988) and Herbig & Leka (1991).

Prior to this work, Chlewicki et al. (1987) found the strong features at 5766.1, 5772.4 and 5775.8 Å in spectra of CygOB2#10 (09.5Ia), CygOB2#5 (O7Ia) and HD207198 (O9Ia) and noticed the shoulder at λ5789. We confirm that these are diffuse interstellar bands and not weak stellar or atmospheric lines.

As a further check on the new DIBs, we have verified that some of the features can be discerned in spectra taken with other instruments and telescopes and by different observers, although the individual spectra do not permit a definite identification. Herbig (1975) noted: " ... there is a suggestion of further structure within λ5778 in HD183143 and HD168625...". The features are

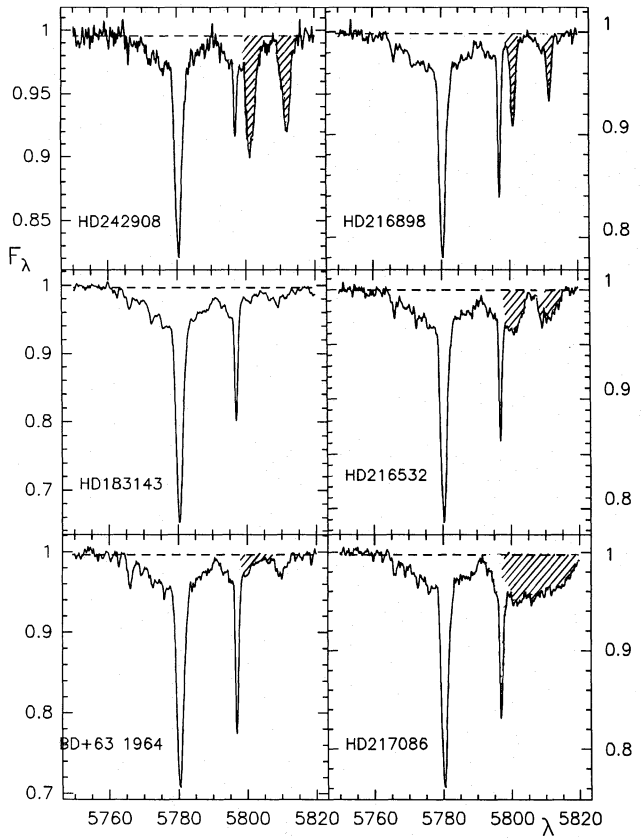

Fig. 2. Some individual spectra of reddened B stars (left) and reddened O stars (right) with a range of stellar rotational velocities. Stellar lines are hatched. The B–type spectrum is made up of the spectra of HD183143 (80), HD38131 (20), HD37367 (16), BD+31 643 (34) and BD+63 1964 (15). The O–type spectrum is made up of the spectra of HD15558 (23), HD216898 (24), HD239729 (26). The value between brackets is the weight factor, which was taken to be E_{B-V} /rms^2, and is given in units of 10^3 mag Å^{-1}

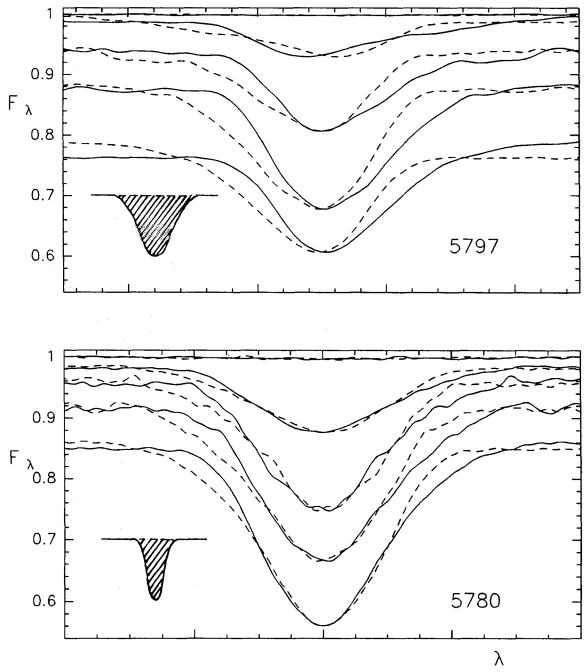

Fig. 3. Profiles of λ5797 and λ5780, shown together with their mirror image reflected around the central position of a Gaussian profile fitted to the DIB. Asymmetry is present in both bands. From top to bottom these are the stars: HD32630, HD216898, HD239729, BD+631964, HD183143. The instrumental resolution of 0.3 Å is indicated

obviously present in high S/N CCD spectra published by Benvenuti & Porceddu (1989, Fig. 1a), Krelowski & Walker (1987, Fig. 3), Krelowski (1989, Fig. 2), Josafatsson & Snow (1987, Fig. 1 – HD281159) and Chlewicki et al. (1986, Fig. 1a – Cyg OB2# 12). The scale of the plots in the latter two publications allows one to recognize the features in the most reddened stars only. The spectra of Snell & Vanden Bout (1981) show the features at 5775.8 and 5784.9 Å. Finally they can be recognized in the spectrum of HD50064 by Herbig & Leka (1991).

A well known feature is the asymmetry in λ5780 and λ5797 (Wu 1972; Savage 1976), which is shown in Fig. 3 by overlaying mirror images (dashed lines) obtained from a reflection in the centroid of the fitted Gaussian profile. λ5797 is asymmetric towards the red with no obvious peaks in the profiles. λ5780 is asymmetric to the red in the wing of the band, but has a shoulder on the blue side close to the band peak (λ5779/6). The asymmetry stands out clearly in the spectra of Snell & Vanden Bout (1981). This feature is responsible for the reported profile variations of λ5780 (notably absent in ν Cep). Westerlund & Krelowski (1988) proceeded by decomposing each profile into five Gaussian components. We are not able to confirm the other three positions, those at 5779.1, 5781.5 and 5792.3 Å, because of our lower resolution. We note that these are not outstanding in the individual spectra and are not included in Table 1.

3.2. *Interrelationships*

Having established the new DIB structure, we follow Chlewicki et al. 1986 and Krelowski & Walker (1987) in searching for family patterns among the strongest features. Because of the limited S/N in the individual features, we restrict ourselves to the question which features follow λ5780 respectively λ5797.

We have measured the equivalent width (W):

$$W = \Sigma_{i=1}^{n}\left(\frac{I_i^b - I_i}{I_i^b}\right)\Delta\lambda \qquad \sim \lambda^2\, N\, f \qquad (1)$$

where the summation is over the n pixels that record the feature, $\Delta\lambda$ = 0.1 Å/px, I^b is the chosen baseline for a given spectrum I, N is the column density of the carrier and f the oscillator strength (in a molecular carrier hypothesis). In each spectrum we chose a baseline consistent with the one chosen in the spectrum of HD183143, where the baseline was taken linear between two points of minimum optical depth in the profile. The strength of the broad DIBs is estimated from the depth of the profile at 5778.0 Å and 5796.0 Å respectively (Table 2).

In Figs. 4 and 5, we compare the intensity of each feature with that of λ5780 and λ5797. In Table 3, the correlation coefficients are given, and each feature is assigned to either 5780 or

Table 2. Table of equivalent widths (mÅ) and profile depths for 22 reddened stars and 9 slightly reddened reference stars. The error in the equivalent width is $\Delta W \simeq \mathrm{rms}\sqrt{2\,\Delta\lambda\,\mathrm{FWHM}}$, where the tabulated value of rms is the root-mean-square value per pixel and $\Delta\lambda$ is 0.1 Å.

STAR	SpT	E(B-V)	66	73	76	780	AC78	89	797	AC96	RMS	W6284	A6281	W6269	A6271	RMS
HD15558	O5III	0.83	25	22	26	452	0.034	15	129	0.026	0.006	397	0.069	48	0.031	0.006
HD30614	O9.5Ia	0.30	4	6	3	111	0.010	2	45	0.004	0.004	47	0.028	19	0.007	0.007
HD34078	O9Vn	0.52	7	17	14	138	0.013	6	43	0.012	0.005	145	0.031	25	0.012	0.006
HD36879	O7.5III	0.50	8	16	15	291	0.025	8	53	0.019	0.005	315	0.036	27	0.017	0.006
HD37367	B2V	0.40	11	28	14	417	0.030	5	85	0.021	0.005	367	0.066	47	0.018	0.003
HD38131	B1III	0.51	14	26	18	386	0.027	7	85	0.022	0.005	408	0.067	61	0.018	0.008
HD154445	B1.5V	0.42	13	22	4	164	0.014	7	53	0.011	0.006	136	0.026	38	0.007	0.003
HD166937	B8Ia	0.24	20	24	6	243	0.016	13	70	0.016	0.005	206	0.039	28	0.010	0.003
HD183143	B7Ia	1.28	32	44	23	721	0.059	23	178	0.047	0.004	681	0.126	117	0.045	0.003
HD190603	B1.5Ia	0.72	11	6	7	326	0.026	6	70	0.022	0.005	245	0.067	27	0.011	0.003
HD192281	O5V	0.70	27	10	10	269	0.016	7	103	0.020	0.005	211	0.039	38	0.011	0.003
HD193682	O5V	0.83	25	18	14	376	0.029	10	73	0.025	0.006	382	0.078	35	0.022	0.010
HD199216	B2III	0.74	14	8	15	186	0.011	9	97	0.011	0.007	117	0.038	30	0.015	0.007
HD209339	O9V	0.36	11	22	7	221	0.015	10	62	0.015	0.004	170	0.050	30	0.015	0.004
HD216532	O8V	0.86	20	24	14	431	0.033	14	119	0.026	0.005	369	0.056	51	0.024	0.006
HD216898	O9V	0.85	24	28	8	440	0.033	11	141	0.023	0.006	359	0.057	62	0.018	0.006
HD217086	O7V	0.95	27	25	22	495	0.036	13	144	0.042	0.006	404	0.075	54	0.028	0.004
HD239729	O9V	0.66	9	15	5	187	0.012	5	74	0.008	0.005	163	0.026	23	0.016	0.012
HD242908	O4V	0.60	7	14	13	356	0.027	14	48	0.024	0.011	276	0.066	<10	<0.010	0.034
BD+31 643	B5V	0.85	13	21	20	259	0.020	8	78	0.012	0.005	168	0.036	40	0.010	0.010
BD+60 497	O6V	0.89	24	26	19	395	0.031	17	122	0.020	0.009	358	0.062	61	0.016	0.016
BD+63 1964	B0.5I	0.95	56	24	19	649	0.045	17	224	0.036	0.008	431	0.074	63	0.028	0.008
HD22928	B5III	0.04	1	1	1	28	0.003	2	8	0.000	0.001	24	0.006	4	0.000	0.001
HD32630	B3V	0.02	0	0	0	<8	0.000	0	<1	0.000	0.001	106	0.024	16	0.011	0.003
HD34085	B8Iae	0.00	0	0	0	<13	0.000	0	<6	0.000	0.003	0	0.000	<6	0.000	0.002
HD35468	B2III	0.01	0	0	0	<0	0.000	0	<2	0.000	0.004	--	-.---	--	-.---	-.---
HD37742	O9.5Ib	0.09	0	0	0	21	0.002	0	<2	0.000	0.002	35	0.004	<6	0.000	0.006
HD47839	O7V	0.08	0	0	0	<16	0.000	0	<2	0.000	0.004	--	-.---	--	-.---	-.---
HD199081	B5V	0.01	0	0	0	16	0.000	0	<1	0.000	0.003	--	-.---	--	-.---	-.---
HD205021	B1III	0.12	0	0	0	<10	0.000	0	<2	0.000	0.003	--	-.---	--	-.---	-.---
HD214680	O8III	0.11	7	6	2	50	0.007	6	15	0.004	0.002	41	0.014	9	0.004	0.002

5797 (bold entry). To good approximation the observational errors in W5780 and W5797 are similar, and are small compared to those of the other features. Thus, the correlation coefficients can be compared directly.

To our surprise, the background λ5796 does follow λ5780 better than λ5797 (in agreement with Chlewicki et al. 1986). Of the weak features, only λ5766.1 follows λ5797. Other, more subtile, variations in the profile may exist. Note, for example, the relative strength of some features in the spectra of BD+63 1964 and HD217086 with respect to HD183143 (Fig. 2). While the narrow features are more pronounced in the former stars, the shoulder that consists of the features λ5787.5 and λ5788.8 is not. In addition, we already mentioned that the feature λ5779.6, which is a shoulder on the strong λ5780, has been shown to vary from one line of sight to another (Snell & Vanden Bout 1981). However, this needs confirmation because it depends heavily on the spectrum of ν Cep.

We do not confirm that λ5778 is member of a separate family (Josafatsson & Snow 1987; 9 stars - probably not significant) nor that λ5797 follows E_{B-V} more closely than λ5780 (Chlewicki et al. 1986; Herbig 1975). Herbig found r=0.85 for λ5780 vs. E_{B-V}, in good agreement with our value, but r=0.98 for λ5797 vs. E(B-V). Benvenuti & Porceddu (1989) found only r=0.62 for λ5780 vs. λ5797. The discrepancies in the absolute values for the correlation coefficients reflect selection effects and differences in observational errors.

Table 3. Correlation coefficients for each of the features with λ5780 and λ5797. The highest value for the correlation coefficients is given as a bold number. The correlation coefficients are derived from data of 26 stars without allowing for observational uncertainties.

	W5780	W5797	E(B-V)
W5766.1	0.82	**0.93**	0.74
W5772.3	**0.82**	0.73	0.68
W5775.8	**0.79**	0.73	0.80
A5778	**0.99**	0.86	0.85
W5780.4	**1.00**	0.91	0.85
W5788.8	**0.85**	0.80	0.78
A5796	**0.96**	0.85	0.83
W5797.0	0.91	**1.00**	0.86

4. The 6284 window

The diffuse band λ6284 is analysed following the same procedure as for λ5780.

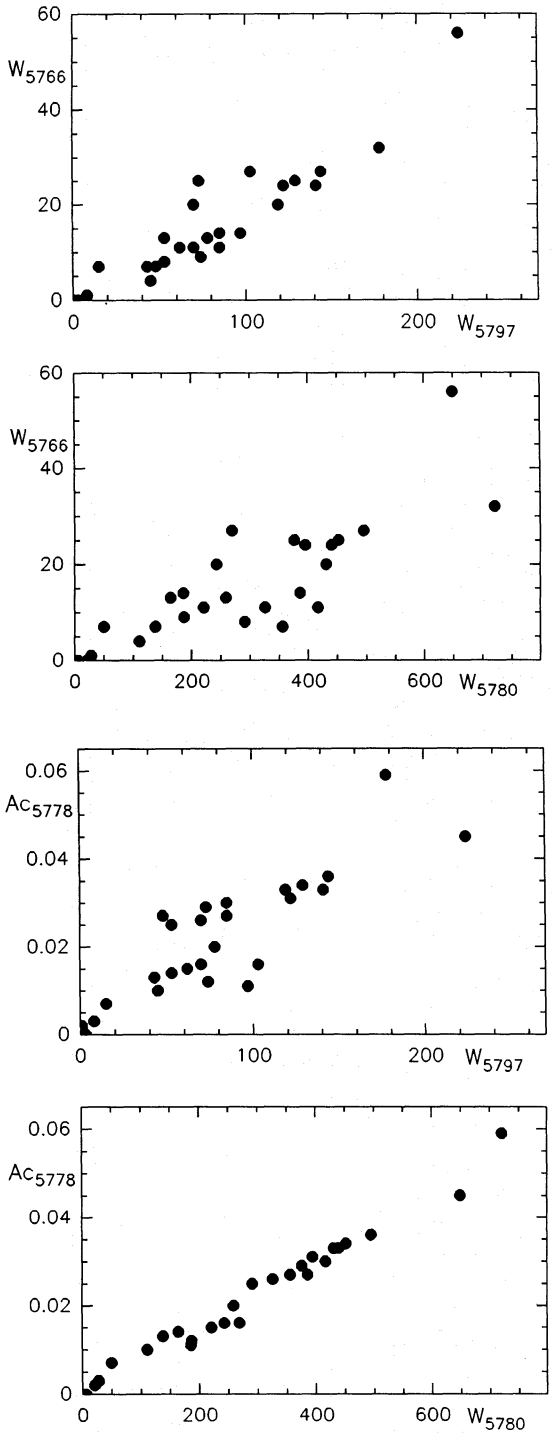

Fig. 4. A comparison of the background λ5778 and the strong λ5766 with the two main DIBs for those lines of sight for which the features could be measured. Note that λ5778 follows λ5780 and that λ5766 follows λ5797 (Compare: Fig. 2)

4.1. New diffuse interstellar bands

The established DIBs between 6220 and 6300 Å are those at λ6269 and λ6284. Chlewicki et al. (1986) discussed a possible DIB at λ6234, which is very prominent in our data. In addition, there are a number of weaker features, listed in Table 4.

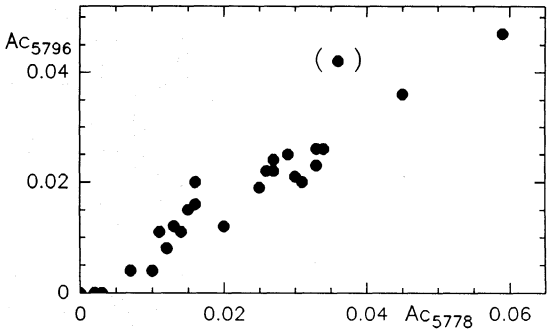

Fig. 5. A comparison of the depth of the background λ5796 and the background λ5778. The deviating point is HD217086, which has heavy *C*IV stellar line contamination

Most striking is the shape of the λ6284 feature itself. Figure 6 shows a S/N=380 spectrum obtained from averaging the spectra of several O and B type stars as before. O-stars: HD207189 (79), HD209339 (44), HD216532 (35) and HD216898 (34). B-stars: HD183143 (151), BD+63 1964 (24), HD154445 (34), HD190603 (79), HD37367 (34). Note that the B-star spectrum is dominated by HD183143. Some individual spectra are shown in Fig. 7.

As Fig. 8 shows, λ6269 is asymmetric towards the red and λ6284 has an asymmetry, like λ5780, with a wing to the red and a shoulder slightly to the blue of the peak center. We have added the approximate position (6283.90 Å) in the list of Table 4, anticipating the similarities between λ5780 and λ6284 discussed in the next section. Again, Westerlund & Krelowski (1988) decomposed the average profile in a number of Gaussian terms, but the components do not stand out in the individual spectra and were not included in Table 4 for that reason.

The λ6284 DIB seems to be a feature superimposed on a broad background labelled λ6281 in Fig. 6. The background has a short wavelength wing which overlaps with λ6269, which may have a similar but weaker background. This structure was noticed recently by Herbig & Leka (1991) from high S/N spectra. We notice that the broad background underlying λ6284 is not a smooth Lorentzian shaped profile, but shows an asymmetry and a series of shoulders. There is a DIB at 6278.3 Å. These features were found consistently in high S/N spectra of BD+63 1964, HD38131, HD37367, HD217086, HD209339 and HD183143. Figure 9 shows the spectrum of HD183143 at a somewhat higher spectral resolution of R=65000, i.e. $\Delta\lambda$ = 0.0097 Å. The features stand out clearly.

The features can be recognised in spectra taken by others with other telescopes. Nice examples are those of HD152249 and HD168076 shown by Benvenuti & Porceddu (1989), and HD183143 shown by Herbig & Leka (1991). Note that the spectra of HD164794 and HD165024 of Benvenuti & Porceddu (1989) also show the complex structure.

4.2. Interrelationships

Once identified, we have measured the strongest features from all our program stars (Table 2), by applying the same procedure

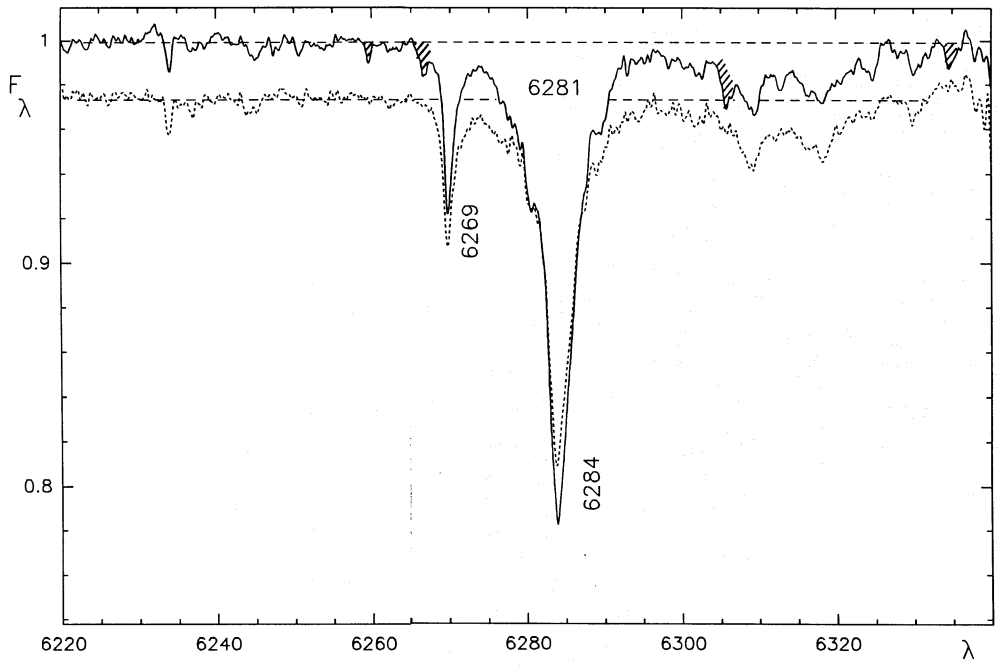

Fig. 6. High S/N average profiles of the 6284 window at 0.3 Å resolution, obtained by averaging the spectra of several B stars (upper curve) and O stars (lower curve)

as for the 5780 window: a Gaussian profile was fitted to the main absorptions of λ6269 and λ6284, with a baseline at the point where the broader background merges with the main feature. The depth of the broad features was measured at 6271.5 and 6281.1 Å (away from the position of the strongest O_2 lines).

In Fig. 10 the equivalenth widths of the weak profile features are compared with the main features λ6284 and λ6269. Benvenuti & Porceddu (1989) noted that λ6269 behaves independently from λ6284. Note that the background λ6271 underlying λ6269 correlates slightly better with λ6284 than with λ6269. The weak feature λ6278.3 could only be measured in 14 stars with high enough signal-to-noise. The low value in the correlation coefficients reflect the observational errors. The few data indicate a better correlation with λ6284 than with λ6269.

5. Tentative link of 5780 and 6284

Having studied the two windows separately, we have reached the situation where we can compare them.

The first argument for a link between λ5780 and λ6284 is the close correlation in equivalent widths from one line of sight to another (r=0.97, Fig. 11). A second argument is that the shape of the λ5780 and λ6284 complexes are very similar: Fig. 10 shows both profiles of HD21389 (A0Iae). The common features are marked. This similarity boils down to: 1) the presence of a background feature underlying λ5780 and λ6284; 2) the good correlation of the background with the main feature; 3) the same asymmetry shown by the main features, with a shoulder on the blue side of the peak and a red wing; 4) the presence of a narrow feature on the blue wing of the broad feature; 5) a sharp onset of the red side of the broad feature; 6) two features on the blue and red side of the main peak that form a plateau on which the main features are superposed; 7) a similarity in the relative position of feature and shoulders (Fig. 10), where the frequency shift between the DIBs 4, 6, 10, 11 and 13 of Table 1 is 10.2, 13.8, 13.4 and 11.7 cm^{-1} respectively, and the frequency shift between the DIBs 6, 7, 9, 10 and 11 of Table 4 is: 6.1, 8.5, 8.5 and 4.2 cm^{-1} respectively.

Summarizing, we conclude that λ5772.4, λ5775.8, the main λ5780, λ5784.9, λ5788.9 and the background λ5778 form a related structure. This structure is similar to that of λ6278.3, λ6280.7, the main λ6284, λ6287.2, λ6288.9 and the background λ6281 (Fig. 10).

Table 4. New and known diffuse band features. Each number in column 2 refers to a tentative corresponding DIB in the list of the 5780Å window of Table 1 (see Section 6). Listed values are the DIB parameters measured for HD183143 (see Table 1).

		λ_c (Å)	ν (cm^{-1})	FWHM (Å)	W (mÅ)	A_c	notes
1.	2	6233.8	16037.2	0.5	12	0.020	=λ6234
2.	-	6236.4	16030.5	0.5	6	0.012	
3.	-	6244.8	16008.9	1.7	25	0.014	
4.	17	6269.71	15945.3	1.09	117	0.107	=λ6269
5.	16	6271.1	15941.8	5.	200	0.045	=λ6271
6.	4	6278.3	15923.5	0.9	12	0.018	
7.	6	6280.7	15917.4	11.	–	0.126	
8.	8	6283.9	15909.3	-.-	–	-.–	shoulder
9.	10	6284.04	15908.9	2.86	681	0.272	=λ6284
10.	11	6287.2	15900.9	1.0	–	0.010	
11.	13	6288.9	15896.7	1.0	–	0.021	
12.	18	6309.1	15845.8	4.8	60	0.021	
13.	-	6316.4	15827.4	20.	46	0.021	=λ6314
14.	20	6318.1*	15823.2	3.7	32	0.016	
15.	22	6324.6	15806.9	1.3	24	0.014	
16.	23	6329.6	15794.4	1.5	28	0.018	

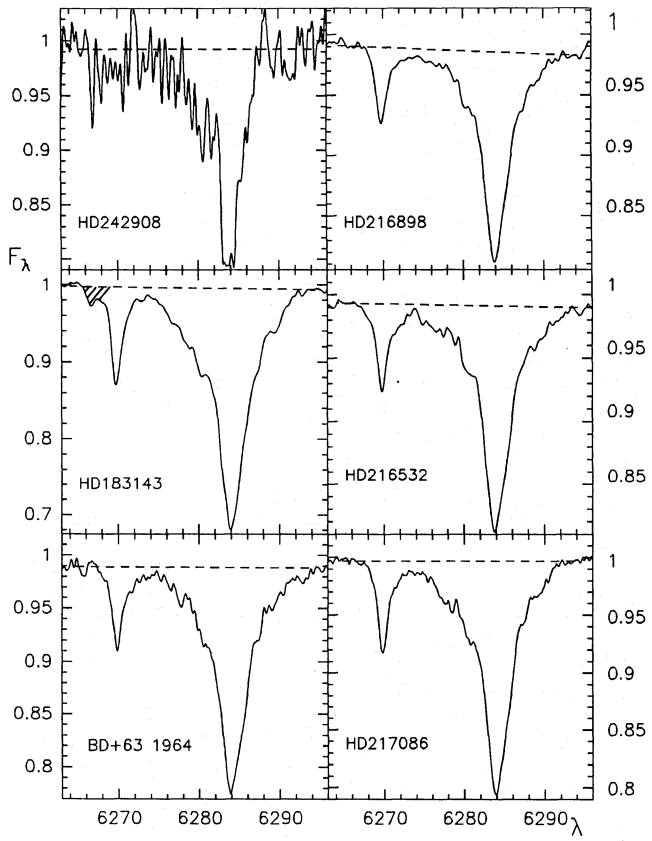

Fig. 7. Some individual spectra, as in Fig. 2

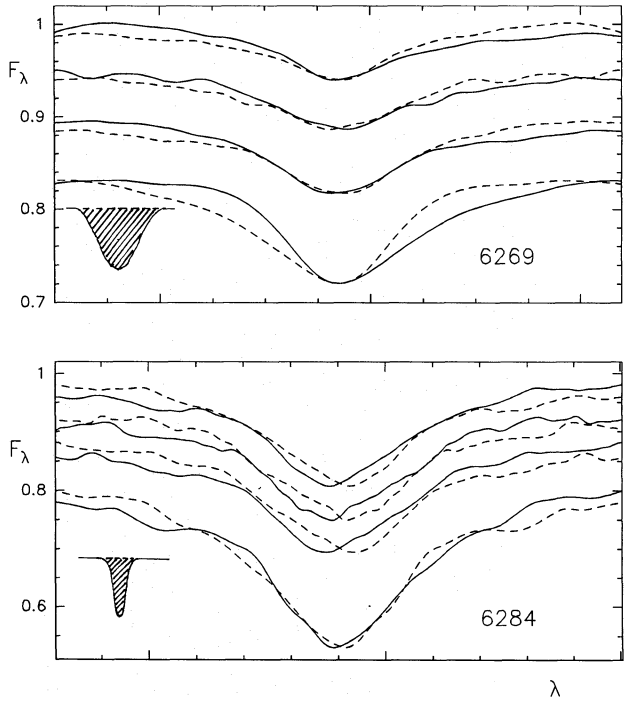

Fig. 8. Asymmetry in λ6269 and λ6284 DIBs, for the same stars as in Fig. 3 (but without the non-reddened HD32630)

However, note that the frequency shift between the features is a factor of ~1.8 smaller in λ6284 while the main peak of λ6284 is broader than λ5780 by a factor of 1.10 in cm^{-1}.

Table 5. Pattern of correlation coefficients (N=26).

	W6284	W6269	E(B-V)	
W6269	0.88	**1.00**	0.80	
A6271	**0.90**	0.87	0.83	
A6281	**0.94**	0.82	0.82	
W6284	**1.00**	0.88	0.81	
W6278.3	**0.68**	0.50	0.56	(N=14)

Table 6. Pattern of correlation coefficients (N=26), compared to the values derived by resp. Chlewicki et al. (1986) and Benvenuti & Porceddu (1989).

	this work	Chlew.'86	BenPor'89
W5780 - W6284	0.97	0.97	0.77
W5780 - W6269	0.86	0.83	0.57
W5797 - W6284	0.82	0.46	0.57
W5797 - W6269	0.85	0.69	0.32

The equivalent widths of the main features are in a ratio of W6284/W5780 = 0.95. If the features had equal oscillator strength (Eq. 1), this ratio would be 1.18.

6. More speculative links between the windows

6.1. Similarities between the λ6280 and λ5780 windows

This paragraph discusses some more speculative associations between various features.

First, there may be a similar relationship between λ6269 and λ5797 as for the λ6284 and λ5780 DIBs, although the evidence is much less compelling. A possible relationship of these two features is based on the following arguments. 1) both bands are well correlated. However, the correlation of λ6269 with λ5780 is found to be as good as that with λ5797 (Fig. 11); 2) both bands show a pronounced asymmetry toward the red, which is not characteristic for DIBs; 3) the wavelength FWHM of the lines are in a ratio of 1.11, which is very close to the expected value if the width in frequency is the same (1.088); 4) both bands seem to be superposed on a weak background absorption.

The ratio of their equivalent widths (0.66) is less than the value expected from Eq. 1 for equal oscillator strength.

With the bold assumption that the frequency difference between λ5766.1 and λ5797 is the same in the 6284 window, we should expect a DIB at 6233.6 Å relative to λ6269. This is within the observational uncertainty of only 0.2Å in agreement with the well established λ6233.8 Å.

Using the same argument, starting from λ5780, we locate the DIB corresponding to λ5809 DIB (which is in the λ5780 family) at 6318.1 Å, at which a similarly shaped DIB is found. λ6309.1, which is of the same strength, should have an associated feature at about 5801.6, which is close to a (stellar line contaminated) DIB. Also the weak λ5814 and λ5818 may have a counterpart

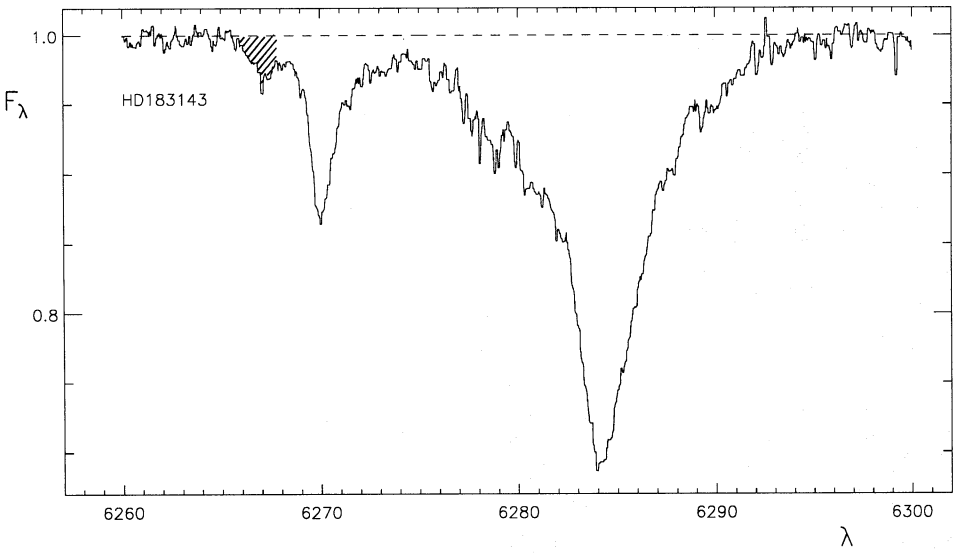

Fig. 9. Spectrum of HD183143 at a resolution of $\Delta\lambda$ = 0.0097Å. The same optical system was used, but with a grating of 1200 lines/mm at 2nd order (grating no. 5; Gillet 1990). The wavelength scale is in the heliocentric rest frame

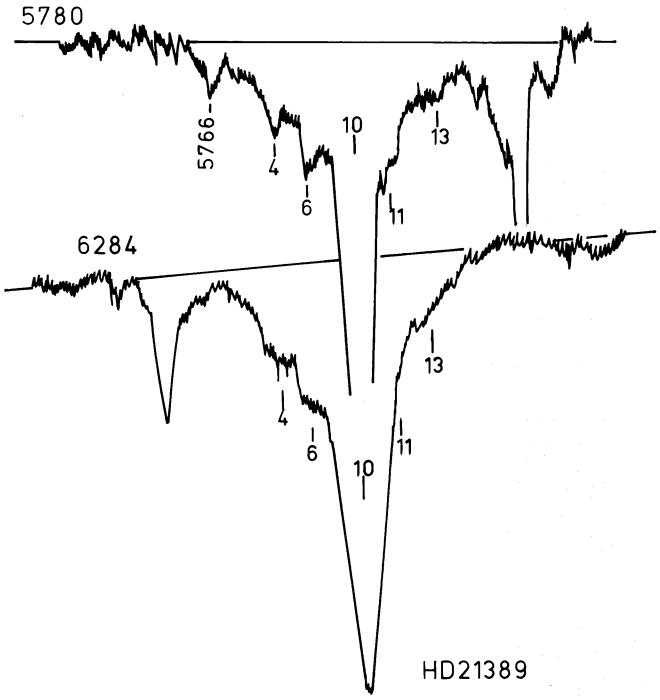

Fig. 10. Comparisson of the profiles of the bands in HD21389. The features in common are marked. The intensity scale and wavelength scale are in arbitrary units

in λ6324 and λ6329.6. The reason why we insist on the mere possibility of such links is given in the discussion below.

6.2. Similarities between the λ6820 and λ5780 windows

A final remark, and possibly unrelated to the previous, concerns what we consider a highly speculative link. Figure 12 compares our series of weak DIBs in the blue wing of λ5778 with the series of weak DIBs found by Herbig (1988) in a window near 6820 Å. This spectrum was obtained at O.H.P. by similar techniques. If the wavelength scale of the 6820 Å window is compressed by an arbitrary factor of 5.1, then it is possible to match all strong DIBs of Herbig's (1988) series with the weak features in the λ5778 profile, where we note a similarity in relative DIB strength as well as in position.

There is a more than fair possibility that the correspondence is merely coincidental. However, it is not completely out of the question that both structures could have the same origin. Of course, a more extended comparative study, on a DIB to DIB basis, is needed before any relationship is proven.

7. Discussion

We have found that the two strongest DIBs, λ5780 and λ6284, have complicated profiles with several structures. The similarity in structure reduces the possibility that the features are a mere chance superposition of unrelated absorptions. This is consistent with intrinsic structure in the absorption profiles, although it does not prove it. We now assume that the structure is real and discuss what kind of transitions may account for the position and shape of the features and the possible link between λ5780 and λ6284.

The mid-infrared emission bands are ascribed to dehydrogenated and partially ionised big (40-100 C) molecules, more specifically Polyaromatic Hydrocarbons (PAH; Léger & Puget 1984; Allamandola et al. 1985), for which abundances are high. Since ionized PAHs have sharp transitions in the visual (e.g. Shida & Iwata 1972; Salama & Allamandola 1992), it is most likely that the DIBs are caused by the subset of these molecules that are ionised (Van der Zet & Allamandola 1985; Crawford et al. 1985; Léger & d'Hendecourt 1985). Because until now the DIBs have not been identified with any certainty we keep open the possibility that some other related molecules are responsible, e.g. radical sidechains on PAHs (Donn 1968) or dehydrogenated PAHs.

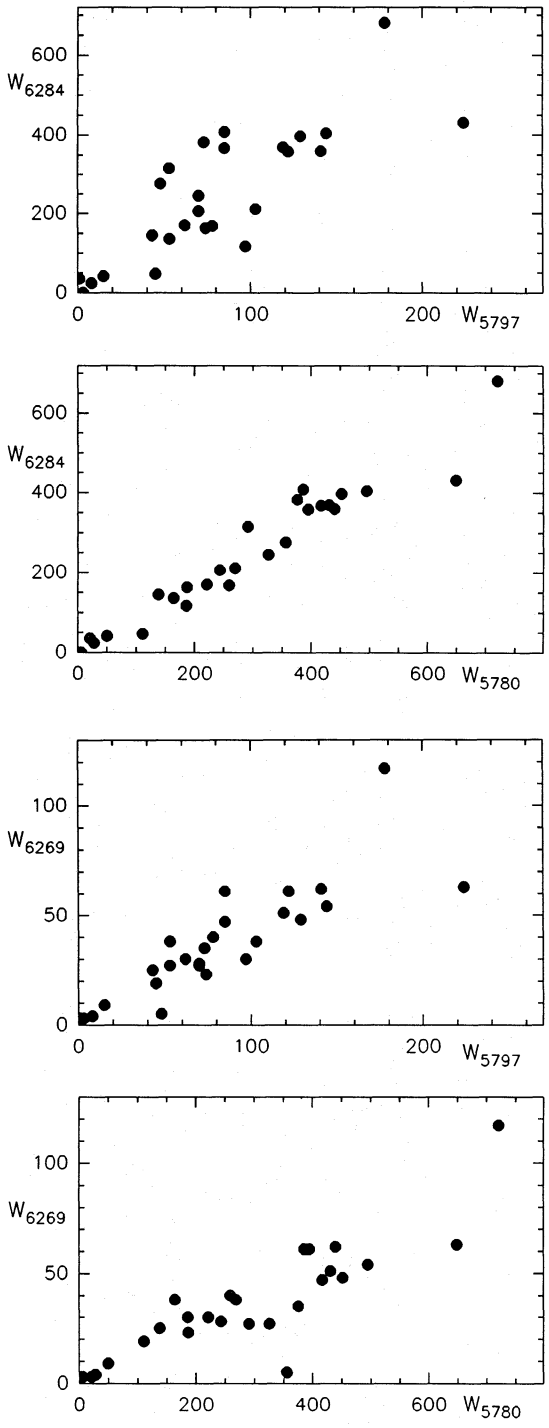

Fig. 11. A comparison of λ6284 and λ6269 with the two main DIBs in the 5780 window: λ5780 and λ5797. Note that λ6284 follows λ5780. λ6269 only shows discrepant behaviour for star HD242908. Its spectrum is very noisy, however, but does seem to indicate a weak λ6269 (Fig. 7)

7.1. Vibronic transitions

The position of DIBs in the visible and near-IR argues for a (dipole allowed) electronic transition. In the interstellar medium conditions are such that the molecules are found in the ground electronic state and usually also in the ground vibrational state (some notable exceptions are given below).

Families of electronic bands occur because coupling between electronic and vibrational states results in the excitation of a series of excited vibrational states when there is a change in geometry from ground to excited state along the coordinate of a normal vibrational mode. The intensity of the transitions are governed by Franck-Condon factors. λ6284 and λ5780 may be part of such a vibrational progression. There are no obvious other candidates between λ6284 and λ5780, indicating that the vibration involved has a frequency of order of the difference between both lines, i.e. 1386.1 cm^{-1}. λ5368 (Herbig 1975; Jenniskens & Désert 1992) is a possible third member (1328 cm^{-1} above λ5780).

We note that the frequency difference between λ5780 and λ6284 corresponds to λ = 7.214 μm, which is of the order of a typical C=C stretch vibrational frequency and graphite lattice vibrational modes. Interstellar dust in regions with a strong UV field shows a broad infrared emission band between 6.8 and 9.0 μm, peaking at 7.7 μm (e.g. Russell et al. 1977; Bregman et al. 1989). Similarly, λ5797 and λ6269 are 1300.9 cm^{-1} apart, which is λ = 7.689 μm, close to the peak of the infrared emission. This emission is thought to be due to C=C vibrations in polycyclic aromatic hydrocarbons (PAH) or small amorphous carbon grains (Léger & Puget 1984; Allamandola et al. 1985). Similar shifts apply to all of the features that were linked in the previous paragraph. This is consistent with the presence of vibrational progressions in carbon containing molecules, but does not prove it.

Electronic excitation of large molecules does not change the binding forces very much, and consequently vibrationless (0_o^o) transitions are favoured. Thus, a vibrational progression (ν_o^1, ν_o^2,...) is somewhat unexpected. The notation stands for zero quanta in the initial state and 1 quantum is in the final state of mode number ν. Small PAHs, like Naphtalene and Coronene, are found to have vibrational progressions even at 10K (Salama et al. 1992; Ehrenfreund et al. 1992).

7.2. Rotational broadening

Any vibrational progression should consist of absorptions with similar rotational structure and be in the same family of DIBs (Danks & Lambert 1976). λ5780 and λ6284 are in the same family. But is the structure observed in these profiles due to rotational broadening?

If one of the three prinicipal moments of inertia ($I_a, I_b, I_c, \sim mr^2$) in polyatomic molecules is large enough, there will be a significant population of the rotational levels in the ground state, even at the kinetic temperatures of T=10-100 K that are typical for diffuse clouds. In diatomic molecules, optical selection rules $\Delta J = -1, 0, +1$ generate at most three bands of rotational lines (P, Q and R branch respectively). In polyatomic molecules, the profiles are superpositions of many such PQR branches with an origin that shifts with J. Depending on the difference in moment of inertia in initial and excited state, band inversions may occur in the P or R branch, leading to accumulation of absorption

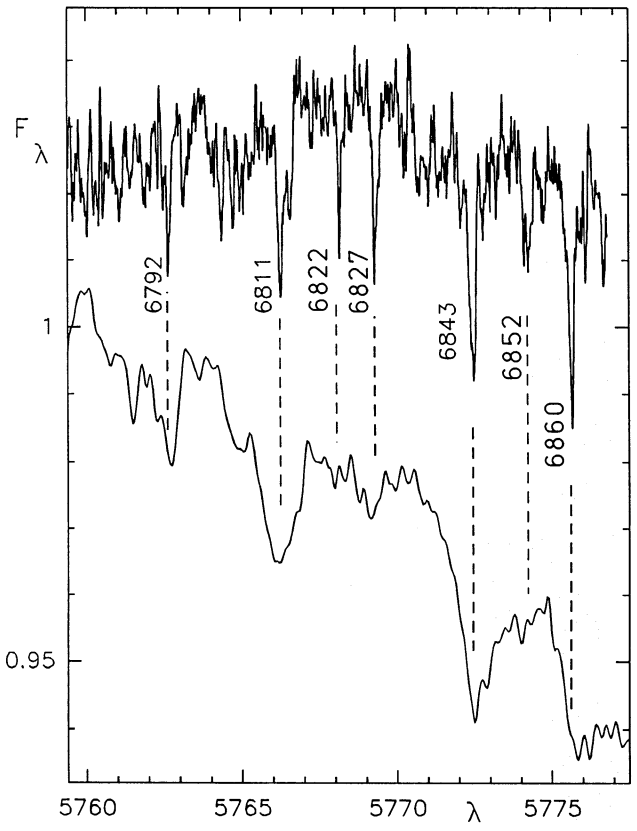

Fig. 12. A comparison of the spectrum of HD183143 near 6820 Å with the blue side of λ5778 for the same star. By compressing the wavelength scale by an arbitrary factor of 5.1, it is possible to match all strong DIBs of Herbig's 1988 series, both in position as in strength

features and sharp cut-offs. Also, regular patterns due to concentrations of Q-branch lines can occur. This can cause structure in the profiles of molecules with significantly different I_a, I_b and/or I_c.

Some features of the complex profiles discussed in this paper do have characteristics of rotational structure. Notably the shoulders on the red side of λ5778 resemble R-band inversions (red shading). Similarly, the peaks on the blue side resemble structure due to Q-branch lines. Alternatively, Danks & Lambert (1976) showed that the central peak, λ5780 is fitted well by a symmetric rotor at T=50K with a largest rotational constant A (= $h/8\pi^2 I_a$) of about 0.20 cm^{-1}, including the shoulder at λ5779.6. The shoulder then would be due to the P branch. The possible absence of the shoulder in (ν Cep) (Snell & Vanden Bout 1981) might be due to unusual low level rotational excitation. But the whole profile (λ5780, λ5778, and the new features) is not understood in terms of rotational structure alone. Also, if λ6284 and λ5780 are in the same vibrational progression, then it is not understood why λ6284 is 10% broader and the features are a factor of 1.8 closer together.

The width of the band follows in first order from: E = 3/2kT = AJ(J+1) and the energy difference between two lines: $\Delta\nu = \Delta A\ J^2$ - 2AJ (neglecting K terms, assuming LTE), which results in $\Delta\nu \sim 1.44\sqrt{B\,T}$, wher B scales with I^{-1}. The width of λ5778 would correspond to at least one of three moments of inertia typical for a small molecule, as small as 3-4 atoms (Danks & Lambert 1976) or highly excited rotational levels. The typical compact PAHs envisaged by Van der Zwet & Allamandola (1985); Crawford et al. (1985) and Léger & d'Hendecourt (1985) have a broadening due to rotation which is less than the width observed for λ5780 (Cossart-Magos & Leach 1990).

We conclude that the profile λ5780/λ5778 is not merely a rovibronic band contour of a large PAH (Van der Zwet 1987).

7.3. The role of lifetime broadening

It is likely that not rotational broadening but a form of lifetime broadening is responsible for the broadening of the lines. Doppler broadening does smooth the rotational band profile but this smoothing is not heavy enough to explain the broad DIBs. Note that other conventional mechanisms like pressure broadening and inhomogeneous broadening are excluded for interstellar gas phase molecules.

Lifetime broadening occurs when the energy in the excited states leaks away quickly to other states. For the relatively photostable molecules responsible for the infrared emission, both transitions to dissociating or ionising transitions are not likely (i.e. pre-dissociation or pre-ionisation). Instead, internal conversion to other electronic states is expected to occur in all molecules with N>5 (Struve 1989). This is a suitable mechanism to protect the molecule from destruction by UV photons (Douglas 1977).

In this case the lines should have a Lorentzian lineshape. The 1/e lifetime $\tau \sim \frac{1}{\Delta\nu} = \frac{2\,\lambda^2}{c\,FWHM}$. Because of the sharpness of the central peak of λ6284, a Lorentzian profile does produce a somewhat better fit than a Gaussian profile. The broadening of λ5780 would correspond to a lifetime of the excited state of $\tau \sim 1 \times 10^{-11}$ s and the broadening of λ5778 equals $\tau \sim 2 \times 10^{-12}$ s, which is not unusually short.

The lifetime broadening mechanism does not account for the observed structure in the profiles, except in certain intermediate size molecules where the density of states at the level of the excited state is small enough to show some clustering of states. The profile then reflects the density of vibrational and rotational states, and the coupling coefficients, in those lower electronic states that are coupled to the excited electronic state. This profile is highly characteristic of the molecule. A transition to a first vibrational excited state instead of the ground state is expected to show a similar (but not the same) band profile (Leach S. & Brechignac P.: priv. comm.).

7.4. Other sources of a multicomponent structure

There are alternative possible mechanisms for the observed structure.

It is possible that part of the structure is due to splitting of a degeneracy in the electronic ground state or excited state (Jahn-Teller). Smith (1977) suggested that the excitation of non-rigid molecules results in broadened (and complex) profiles, because in the ground state the molecules are in different configurations

(which are separated by weak potential barriers). Alternatively, the structure could be due to electronic transitions from different but related molecules with only slightly different structure. Isotope substitution (Chlewicki et al. 1986) probably does not account for the difference in position of the weak lines with respect to λ5780. Although the intensity difference with λ5780 is as expected from cosmic abundance ratio of $^{13}C/^{12}C$, the features are expected on the red side of λ5780 instead of on the blue side.

In polyatomic (N atom) molecules, the range of available transitions is large because of the 3N-6 degrees of vibrational freedom that might be excited (e.g. Struve 1989). If vibrations are excited, then vibrational motion of the nuclei is able to couple electronic states. Due to such vibronic coupling the transition moment to a forbidden state may 'borrow' intensity from a dipole alowed state, so that many more transitions are observable besides the electric dipole allowed transitions. The resulting vibronic spectra are complex and may occasionally show a crowding, like that observed near the vibrationless band of the triacetylene cation (Klapstein et al. 1984).

Finally, large molecules usually have vibrational modes with low wavenumbers. If these are significantly populated in the ground state, excitation to a vibrational state (I) in the upper electronic state results in a sequence of vibrational bands with $\Delta\mu = 0$ (i.e. $0_o^o, I_1^1, I_2^2, \ldots$) because such low wavenumber vibrations are mostly nontotally symmetric (e.g. Hollas 1982). As explained by Duley (1973), there should be some (sub)millimeter transitions with a low frequency cut-off if such (phonon) modes of low frequency are important. Note that the sequence of bands in the 5780 (and 6820) series of bands are not equally spaced and, therefore, do not represent a vibrational ladder of a single low frequency mode.

7.5. Impurity in grains

In the previous discussion we assumed that the carrier is a gas phase molecule. The alternative scenario, that of impurities in grains, cannot be fully discarded (see review by Chlewicki et al. 1986). The absorptions could be due to forbidden transitions of metal ions, which become weakly allowed by the presence of a ligand electric field. The lines of impurity absorptions are broad because of small variations in ligand interaction from site to site. Structure in the profiles occurs because different sites are present in a typical interstellar grain. But the constancy of wavelengths argues against this interpretation.

The profile shown by Duley (1979) does not resemble the one found here. Most elaborate is the assignment by Duley (1982) of DIBs to a series of vibrational overtones ($\Delta\mu$ = +2, +3, ...) and combination bands. The family patterns observed are not consistent with Duley's assignment. The λ5780 and λ6284 bands were assigned to systems with a different origin.

8. Conclusions

We have shown that the two strongest DIBs, λ6284 and λ5780, have complex profiles. Several shoulders and peaks are presented in Table 1 and Table 4 as individual DIBs. Several of these features form a structure which is similar in the two bands. This argues in favour of intrinsic structure in the profiles, but, of course, does not prove it.

The strong correlation in band strength between the two DIBs and their similar structure (Fig. 10) may indicate that they have the same carrier. However, the central peak of λ6284 is a factor of 1.10 broader (in cm^{-1}), while the common features are a factor of 1.8 closer together.

We have discussed several mechanisms for obtaining such structure and broadening, but note that a definitive physical explanation for all the features taken together is lacking. The profile is not merely a rotational-vibrational band contour of a big molecule.

Acknowledgements. We felt great support from the presence of Jacek Krelowski, who visited the Laboratory Astrophysics in Oct.-Dec. 1990, and Xander Tielens, who visited the Leiden Observatory in May-July 1992. The paper has benefitted from many stimulating discussions. Dennis Gillet has introduced us to the telescope and spectrograph at OHP, Michel Dennefeld introduced us to the IHAP reduction package at the Institut d'Astrohpysique de Paris. Henk van de Hulst, Harm Habing, Ewine van Dishoeck, Menno de Groot and Xander Tielens commented on earlier versions of this paper.

References

Allamandola L.J., Tielens A.G.G.M., Barker J.R., 1985, ApJ 290, L25
Benvenuti P., Porceddu I., 1989, A& A 223, 329
Bromage G.E., 1972, Astroph. Space Sci. 15, 426
Bromage G.E., 1987, Q. J.R.A.Soc. 28, 294
Chlewicki G., Van der Zwet P., Van IJzendoorn L.J., Greenberg J.M., Alvarez P.P., 1986, ApJ 305, 455
Chlewicki G., de Groot M.S., Van der Zwet G.P., Greenberg J.M., Alvarez P.P., Mampaso A., 1987, A& A 173, 131
Cossart–Magos C., Leach S., 1990, A& A 233, 559
Crawford M.K., Tielens A.G.G.M., Allamandola L.J., 1985, ApJ 293, L45
Danks A.C., Lambert D.L., 1976, MNRAS 174, 571
Désert F.-X., Jenniskens P., Dennefeld M., 1993, A& A submitted
Donn B., 1968, ApJ 152, L129
Douglas A.E., 1977, Nature 269, 130
Duley W.W., 1973, Nature Phys. Sci. 244, 57
Duley W.W., 1982, Astroph. & Space Sc. 88, 501
Duley W.W., 1979, ApJ 227, 824
Ehrenfreund P., L. d'Hendecourt, L. Verstraete, A. Léger, W. Schmidt, D. Defourneau, A& A 259, 257
Gillet D., 1990, *OHP Notice d'utilisation no.4, Spectromètre Aurelie*, internal publication.
Hayden-Smith Wm., Snow T.P., Jura M., Cochran W.D., 1981, ApJ 248, 128
Heger M.L., 1921, Lick Obs. Bull. 10, 146
Herbig G.H., 1975, ApJ 196, 129
Herbig G.H., 1988, ApJ 331, 999
Herbig G.H., Soderblom D.R., 1982, ApJ 252, 610

Herbig G.H., 1990, ApJ 358, 293
Herbig G.H., Leka K.D., 1991, ApJ, 382, 193
Hollas J.M., 1982, *High Resolution Spectroscopy*, Butterworths, Ch. 6.3
Jenniskens P., Désert F.-X., 1993, "A survey of diffuse interstellar bands", A& A submitted
Josafatsson K., Snow T.P., 1987, ApJ 319, 436
Klapstein D., Kuhn R., Maier J.P., Ochsner M., Zambach W., 1984, J. Am. Chem. Soc., 88, 5176
Krelowski J., Walker G.A.H., 1987, ApJ 312, 860
Krelowski J., 1989, in it Interstellar Dust, IAU Symp. 135, 67
Léger A., d'Hendecourt L., 1985, A& A 146, 81
Merrill P.W., 1936, ApJ 83, 126
Moore C.E., 1945, Contr. Princeton University Obs., no. 20, *A Multiplet Table of Astrophysical Interest*.
Russell R.W., Soifer B.T., Willner S.P., 1977, ApJ 217, L149
Salama F., Allamandola L.J., 1992, Nature 358, 42
Savage B.D., 1976, ApJ 205, 122
Shida T., Iwata S., 1972, J. Am. Chem. Soc., 95, 3473
Smith W.H., Snow T.P., York D.G., 1977, ApJ 218, 124
Snell R.L., Vanden Bout P.A., 1981, ApJ 244, 844
Snow T.P., 1973, AJ 78, 913
Struve W.S., 1989, *Fundamentals of Molecular Spectroscopy*, J.Wiley & Sons.
Van der Zwet G.P., Allamandola L.J., 1985, A& A 146, 76
Van der Zwet G., 1987, in *Polycyclic Aromatic Hydrocarbons and Astrophysics*, eds. A. Léger et al., p. 351
Westerlund B.E., Krelowski J., 1988, A& A 203, 134
Wu C.-C., 1972, ApJ 178, 681

This article was processed by the author using Springer-Verlag TEX A&A macro package 1992.